

A NOVEL BROADBAND COAXIAL PROBE TO CONICAL WIRE TRANSITION AT THZ FREQUENCY

Z. H. Wang, Y. Zhang, R. M. Xu, and W. G. Lin

EHF Key Laboratory of Fundamental Science
School of Electronic Engineering
University of Electronic Science and Technology of China
Chengdu 611731, China

Abstract—In this study, transmission characteristics of a novel THz wire waveguide — conical metal wire with dielectric coating at 0.1–1 THz are studied. The investigation results show that the coated conical wire with virtually low attenuation and high energy concentration is a promising candidate as THz transmission medium. The calculation results agree well with that of simulation such as high frequency structure simulation (HFSS), which is based on the finite element method. In this paper, a novel transition from a coaxial line to the coated conical metal wire is designed. Although coaxial probe excitation has been used in microstrip lines and rectangular waveguides in microwave, millimeter-wave frequency domains, the present study shows that it is also an effective method to excite conical wire at THz frequency. As shown in the investigation results, the return loss of coax-conical wire transition is better than 20 dB from 0.1–0.5 THz, and the insertion loss is as low as 1 dB (the total length is 15 mm). It is a promising THz transition structure.

1. INTRODUCTION

Terahertz (THz), located between the infrared and microwave wave bands in the electromagnetic spectrum, is one of the hot research issues because of its great potential applications in many scientific and technological fields. The interest in THz technology has strongly increased in the last years with diverse applications in the fields of biotechnology [1, 2], spectroscopy [3, 4], imaging [5, 6], etc. Efficient guided THz transmission solutions are still under investigation.

Many kinds of THz waveguides have been presented, such as metal waveguides [7–10], plastic ribbons [11], fibers [12–15]. But those waveguide methods have the disadvantages of high loss, serious group velocity dispersion, and short propagation length. Flexible plastic fiber coated with metal film on the inner surface could also be used to propagate a THz wave, and it has many merits such as high coupling efficiency, convenient realization of single-mode propagation, low cost and attenuation loss [16–18], but it is difficult to fabricate those fibers. With the advantages of low group-velocity dispersion, low loss, and no cutoff frequency, the parallel plate metal waveguide [19–22] is another important THz waveguide method, although the large cross-sectional area limits its applications. In 2004, Wang and Mittleman [23] firstly proposed that cylindrical bare metal wire can be used to confine and propagate a THz wave. Compared with earlier metal tube waveguides [24], a THz metal wire waveguide has the merits of simple structure, low attenuation, and group velocity dispersion [25]. Since then, much theoretical and experimental research has been carried out to study metal wire waveguides. Metal wire waveguides are an interesting research topic for applications in THz imaging and spectroscopy [26–28]. Also, wave propagation has a weak guidance property due to the small electric field in the metal wire [29–31]. There is no guided propagation on a perfect conductor, as there is no field distribution in the conductor [30, 32]. When the generated THz pulses were coupled with the cylindrical conductor (wire), only the dominant transverse-magnetic surface wave mode (TM_{01} : the Sommerfeld wave) was propagated along the wire. Because all the higher modes had very high attenuations, they vanished almost immediately after they were coupled with the wire.

Recently, a conical wire tip was used to launch a THz pulse on a metal wire waveguide by many researchers such as Deibel et al. [33], Jeon et al. [29], Smorenburg et al. [34], etc. It shows higher field intensity than did cylindrical metal wire, because the strongest field was focused at the end of the conical metal wire tip [35, 36]. Compared with the periodically corrugated, grooved metal wire [37] and sharp metal wedge [38], the simple conical metal wire waveguide is much easier to fabricate, and it is suitable for superfocusing of a THz wave [39, 40]. But at terahertz frequencies, due to its strong energy concentration, most energy concentrate on the surface of metal wire, it results in the increase of propagation attenuation. In this paper, based on the conical metal wire waveguide proposed by Jeon et al. [29], we demonstrate a novel THz wire waveguide — conical metal wire with dielectric coating. In part 2, we demonstrate the theory of surface wave propagation along the conical wire at THz frequency. In part 3, the

propagation characteristics of coated conical wire, such as propagation attenuation and energy confinement at 0.1–1 THz will be discussed. The investigation results show that the coated conical wire is a low loss and high energy confinement structure THz transmission line. As we know, how to design an efficient transition is very important. Although coaxial probe excitation has been uses in microstrip lines and rectangular waveguides in microwave frequency domain, the present study shows that it is also an effective method to excite the conical wire at THz frequency. Based on the results above, a novel transition from a coaxial probe to conical metal wire is designed at 0.1–0.5 THz in part 4. The results show that it is a promising transition at THz frequency.

2. SURFACE WAVE PROPAGATION THEORY OF CONICAL METAL WIRE WITH DIELECTRIC COATING

The configuration and structure of the coated conical metal wire waveguide has been shown in Fig. 1. The radius of metal wire decreases from a to a_z and the outer radius of dielectric coating decreases from b to b_z , respectively. ρ is the radius of metal wire and $a_z \leq \rho \leq a$. The THz wave propagation along the z direction. Under the framework of the Sommerfeld model, the dominant propagation surface wave is the azimuthally symmetric TM_{01} mode, and the higher modes have very high attenuations and vanish almost immediately. The field components of the Sommerfeld wave can be written as [32, 41].

In the dielectric coating:

$$E_{ri} = A_i \frac{h}{\gamma_i} [N_0(\gamma_i \rho) J_1(\gamma_i r) - N_1(\gamma_i r) J_0(\gamma_i \rho)] e^{j(\omega t - hz)} \quad (1a)$$

$$E_{zi} = A_i [N_0(\gamma_i \rho) J_0(\gamma_i r) - N_0(\gamma_i r) J_0(\gamma_i \rho)] e^{j(\omega t - hz)} \quad (1b)$$

$$H_{\phi i} = A_i \frac{k_i}{\gamma_i} \sqrt{\frac{\epsilon_i}{\mu_i}} [N_0(\gamma_i \rho) J_1(\gamma_i r) - N_1(\gamma_i r) J_0(\gamma_i \rho)] e^{j(\omega t - hz)} \quad (1c)$$

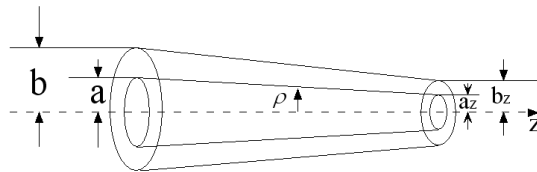


Figure 1. Schematic of a conical metal wire waveguide with dielectric coating.

where A_i is constant. h is the propagation constant of the guided wave and is the same inside and outside the wire. ω is the angular frequency of the electromagnetic wave. ε_i and μ_i are the permittivity constant and permeability constant of dielectric coating. N_0 and N_1 indicate Neumann functions of zero and first order, respectively. J_0 and J_1 indicate Bessel functions zero and first order, respectively. $k_i = \omega\sqrt{\varepsilon_i\mu_i}$ is the wave vector in the material of the coating and $\gamma_i = \sqrt{k_i^2 - h^2}$. $h = \alpha + j\beta$ is the propagation constant of the surface wave.

In the outer free space:

$$E_{r0} = -jA_0 \frac{h}{\gamma_0} H_1^{(1)}(j\gamma_0 r) e^{j(\omega t - hz)} \quad (2a)$$

$$E_{z0} = A_0 H_0^{(1)}(j\gamma_0 r) e^{j(\omega t - hz)} \quad (2b)$$

$$H_{\phi 0} = -jA_0 \frac{k_0}{\gamma_0} \sqrt{\frac{\varepsilon_0}{\mu_0}} H_1^{(1)}(j\gamma_0 r) e^{j(\omega t - hz)} \quad (2c)$$

where A_0 is constant. ε_0 is the dielectric constant of air. $H_0^{(1)}$ and $H_1^{(1)}$ are Hankel functions of the first kind, and zero and first order, respectively. $k_0 = \omega\sqrt{\varepsilon_0\mu_0}$ is the wave vector in the outer free space and $\gamma_0 = \sqrt{h^2 - k_0^2}$.

For the case, the ratio E_z/H_ϕ for the region within the dielectric coating must be continuous at $r = \frac{b}{a}\rho$. Then using Eqs. (1) and (2), the boundary condition at the surface of dielectric coating can be expressed as [41]:

$$\sqrt{\frac{\varepsilon_i}{\mu_i}} \frac{k_i}{\gamma_i} \frac{N_0(\gamma_i \rho) J_0(\gamma_i \frac{b}{a} \rho) - N_0(\gamma_i \frac{b}{a} \rho) J_0(\gamma_i \rho)}{N_0(\gamma_i \rho) J_1(\gamma_i \frac{b}{a} \rho) - N_1(\gamma_i \frac{b}{a} \rho) J_0(\gamma_i \rho)} = j \sqrt{\frac{\mu_0}{\varepsilon_0}} \frac{\gamma_0}{k_0} \frac{H_0^{(1)}(j\gamma_0 \frac{b}{a} \rho)}{H_1^{(1)}(j\gamma_0 \frac{b}{a} \rho)} \quad (3)$$

$$\gamma_i^2 = k_i^2 - k_0^2 - \gamma_0^2 \quad (4)$$

The energy propagating through the area of the transverse plane for $\rho < r < \infty$ can be written as [41]:

$$P = \text{Re} \left[\int_{\rho}^{\infty} E_r(z) H_\phi^*(z) dr \right] \quad (5)$$

The coated conical wire can be considered as constitution of numberless cylinder wire. Therefore, when the THz surface wave propagates on the coated conical wire, the energy distribute in the outer free space can be expressed as [41]

$$P_0 = \text{Re} \left[2\pi \int_{\frac{b}{a}\rho}^{\infty} r E_{r0} H_{\phi 0}^* dr \right] \quad (6)$$

From Eq. (2), Eq. (6) becomes

$$\begin{aligned}
 P_0 &= \text{Re} \left[2\pi A_0 A_0^* \frac{hk_0}{\gamma_0 \gamma_0^*} \sqrt{\frac{\varepsilon_0}{\mu_0}} \int_{\frac{b}{a}\rho}^{\infty} r H_1^{(1)}(j\gamma_0 r) H_1^{(1)}(j\gamma_0 r)^* dr \right] \\
 &= A_0 A_0^* \pi \sqrt{\frac{\varepsilon_0}{\mu_0}} \frac{hk_0}{\gamma_0^4} F \left(\gamma_0 \frac{b}{a} \rho \right)
 \end{aligned} \tag{7}$$

where

$$\begin{aligned}
 F \left(\gamma_0 \frac{b}{a} \rho \right) &= \left(\gamma_0 \frac{b}{a} \rho \right)^2 \left\{ -\frac{2a}{\gamma_0 b \rho} j H_0^{(1)} \left(j \gamma_0 \frac{b}{a} \rho \right) H_1^{(1)} \left(j \gamma_0 \frac{b}{a} \rho \right) \right. \\
 &\quad \left. - \left[H_0^{(1)} \left(j \gamma_0 \frac{b}{a} \rho \right) \right]^2 - \left[H_1^{(1)} \left(j \gamma_0 \frac{b}{a} \rho \right) \right]^2 \right\} \\
 &= \left(\gamma_0 \frac{b}{a} \rho \right)^2 \left[H_1^{(1)} \left(j \gamma_0 \frac{b}{a} \rho \right) \right]^2 \left\{ -\frac{2j}{\gamma_0 \frac{b}{a} \rho} \frac{H_0^{(1)}(j\gamma_0 \frac{b}{a} \rho)}{H_1^{(1)}(j\gamma_0 \frac{b}{a} \rho)} \right. \\
 &\quad \left. - \left[\frac{H_0^{(1)}(j\gamma_0 \frac{b}{a} \rho)}{H_1^{(1)}(j\gamma_0 \frac{b}{a} \rho)} \right]^2 - 1 \right\}
 \end{aligned} \tag{8}$$

Since for large $\frac{b}{a}\rho\gamma_0$ [41],

$$\frac{H_0^{(1)}(j\gamma_0 \frac{b}{a} \rho)}{H_1^{(1)}(j\gamma_0 \frac{b}{a} \rho)} \cong j \quad \text{and} \quad \left[H_1^{(1)} \left(j \gamma_0 \frac{b}{a} \rho \right) \right]^2 \cong \frac{2a}{\pi \gamma_0 b \rho} e^{-2\gamma_0 \frac{b}{a} \rho} \tag{9}$$

then $F(\gamma_0 \frac{b}{a} \rho)$ becomes

$$F \left(\gamma_0 \frac{b}{a} \rho \right) = \frac{4}{\pi} e^{-2\gamma_0 \frac{b}{a} \rho} \tag{10}$$

At the boundary $r = \frac{b}{a}\rho$, the magnetic component H_ϕ can be expressed in terms of the longitudinal current I [42]

$$(H_\phi)_{r=\frac{b}{a}\rho} = \frac{aI}{2\pi b\rho} \tag{11}$$

Substituting Eq. (2c) into (11), and solving for A_0 , we are able to obtain the relation

$$A_0 A_0^* = \frac{a\gamma_0^3}{8\pi k_0^2 b\rho} \left(\frac{\mu_0}{\varepsilon_0} \right) e^{2\gamma_0 \frac{b}{a} \rho} I^2 \tag{12}$$

From Eqs. (7), (10) and (12), the power outside the guide becomes

$$P_0 = \sqrt{\frac{\mu_0}{\varepsilon_0}} \frac{h}{k_0} \frac{aI^2}{2\pi b\rho\gamma_0} = \frac{h}{\omega\varepsilon_0} \frac{aI^2}{2\pi b\rho\gamma_0} \tag{13}$$

The energy distribute in the dielectric coating can be expressed as [42]

$$P_i = \text{Re} \left[2\pi \int_{\rho}^{\frac{b}{a}\rho} r E_{r_i} H_{\phi_i}^* dr \right] = \frac{hI^2}{2\pi\omega\varepsilon_i} \ln \frac{b}{a} \quad (14)$$

Then the total power distribute around the wire is:

$$P = P_0 + P_i = \frac{hI^2}{2\pi\omega\varepsilon_i} \left(\frac{a\varepsilon_i}{b\rho\gamma_0\varepsilon_0} + \ln \frac{b}{a} \right) \quad (15)$$

The conductivity energy loss P_c is found from [42]

$$dP_c = \frac{1}{2\pi\rho} \sqrt{\frac{\omega\mu_c}{2\sigma_c}} I^2 dz \Rightarrow P_c = \frac{1}{4\pi\rho} \sqrt{\frac{\omega\mu_c}{2\sigma_c}} I^2 \quad (16)$$

The dielectric energy loss P_d is obtained from [42]

$$dP_d = \frac{h^2}{2\pi\omega\varepsilon_i} \left(\ln \frac{b}{a} \right) \tan \delta_i I^2 dz \Rightarrow P_d = \frac{h^2}{4\pi\omega\varepsilon_i} \left(\ln \frac{b}{a} \right) \tan \delta_i I^2 \quad (17)$$

The radiation energy loss P_R (the radiation boundary is $r = c$) is obtained from [42]

$$dP_R = \frac{h^2}{2\pi\omega\varepsilon_0} \left(\ln \frac{c}{b} \right) \tan \delta_0 I^2 dz \Rightarrow P_R = \frac{h^2}{4\pi\omega\varepsilon_0} \left(\ln \frac{c}{b} \right) \tan \delta_0 I^2 \quad (18)$$

where $\tan \delta_i$ and $\tan \delta_0$ are the loss tangent of the dielectric material and the air, respectively. σ_c and μ_c are metal conductivity and permeability, respectively. From Eqs. (15)–(18), we can obtain the conductor loss α_c , dielectric loss α_d and radiation loss α_R [42]

$$\left\{ \begin{array}{l} \alpha_c = \frac{P_c}{2P} = \frac{\omega\varepsilon_i}{2\rho h} \frac{\sqrt{\frac{\omega\mu_c}{2\sigma_c}}}{\frac{\varepsilon_i a}{b\rho\gamma_0\varepsilon_0} + \ln \frac{b}{a}} \\ \alpha_d = \frac{P_d}{2P} = \frac{h \ln \frac{b}{a} \tan \delta_i}{2 \left(\frac{\varepsilon_i a}{b\rho\varepsilon_0\gamma_0} + \ln \frac{b}{a} \right)} \\ \alpha_R = \frac{P_R}{2P} = \frac{h \ln \frac{c}{b} \tan \delta_0 \varepsilon_i}{2\varepsilon_0 \left(\frac{\varepsilon_i a}{b\rho\varepsilon_0\gamma_0} + \ln \frac{b}{a} \right)} \end{array} \right. \quad (19)$$

Then, the total propagation attenuation α of coated conical metal wire can be obtained

$$\alpha = \alpha_c + \alpha_d + \alpha_R$$

$$= \frac{1}{2 \left(\frac{\epsilon_i a}{b \rho \gamma_0 \epsilon_0} + \ln \frac{b}{a} \right)} \left(\frac{\omega \epsilon_i}{\rho h} \sqrt{\frac{\omega \mu_c}{2 \sigma_c}} + h \ln \frac{b}{a} \tan \delta_i + \frac{h \ln \frac{c}{b} \tan \delta_0 \epsilon_i}{\epsilon_0} \right) \quad (20)$$

3. SURFACE WAVE PROPAGATION ALONG CONICAL METAL WIRE WITH DIELECTRIC COATING

In this paper, a coated conical copper wire with 10 mm length, whose the radius of metal wire (Copper: 5.8×10^7 S/M) gradually decreases from 250 μm to 15 μm , and the outer radius of dielectric coating (Teflon: $\epsilon_r = 2.05\epsilon_0$, $\tan \delta = 0.001$) gradually decreases from 300 μm to 18 μm , is adopted. The uncoated conical copper wire (Copper: 5.8×10^7 S/M) with 10 mm length, and the radius of metal wire (Copper: 5.8×10^7 S/M) gradually decreases from 250 μm to 15 μm is adopted. The coated cylindrical copper wire with 10 mm length, whose the radius of metal wire is 250 μm , and the outer radius of dielectric coating (Teflon: $\epsilon_r = 2.05\epsilon_0$, $\tan \delta = 0.001$) is 300 μm , is adopted. In this study, the propagation attenuation also was calculated with an HFSS numerical field simulation. The THz Sommerfeld wave is an electric field in the cylindrical wire. The simulation domain was

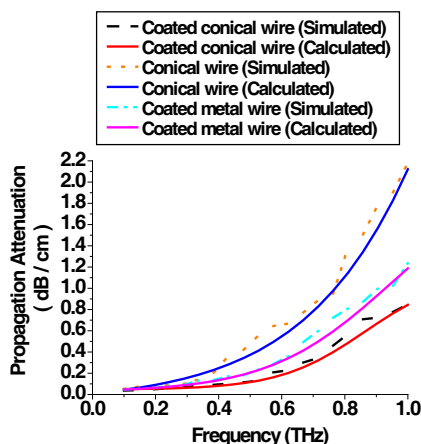


Figure 2. Propagation attenuation of THz metal wire waveguide versus frequency.

bounded by a 4.5 mm-radius and 10 mm-long cylindrical tube, with the wire model located in the center. In this simulation, the plan wave excited on the circular input faces of the cylindrical tube. The outer wall of the domain assumed a radiation boundary condition. The comparisons of propagation attenuation during 10 mm distance between of the coated conical metal wire, uncoated metal wire and coated cylindrical metal wire are shown in Fig. 2.

From Fig. 2, it can be seen that the coated conical metal wire has smaller propagation attenuation than the other two types of THz waveguide from 0.1 THz to 1 THz. And the calculation results are in agreement with the simulation results.

Figure 3(a) shows the ratio of the E field component (the radial distance from the surface of metal wire) at the coated conical metal wire end tip ($a_z = 15 \mu\text{m}$ and $b_z = 18 \mu\text{m}$) to that at the $250 \mu\text{m}$ -radius tip of coated cylindrical metal wire versus frequency. As shown in Fig. 3(a), when the frequency changes from 0.1 THz to 1 THz, the ratio of the E field changes about from 9 to 1.6. From Fig. 3(a), it is clearly that the conical metal wire with dielectric coating has stronger field concentration at the end tip than the coated cylindrical metal wire. Fig. 3(b) shows the ratio of the E field component (the radial distance from the surface of metal wire) at the coated conical metal wire end tip ($a_z = 15 \mu\text{m}$ and $b_z = 18 \mu\text{m}$) to that at the $15 \mu\text{m}$ -radius tip of uncoated conical metal wire versus frequency. As shown in Fig. 3(b), when the frequency changes from 0.1 THz to 1 THz, the ratio of the E field changes about from 1.04 to 1.07. In Ref. [43],

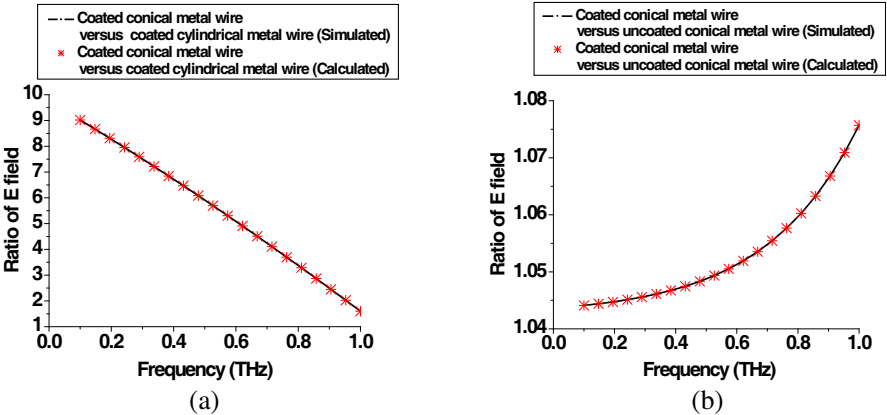


Figure 3. Ratio of the E field component versus frequency. (a) Coated conical metal wire versus coated cylindrical metal wire. (b) Coated conical metal wire versus uncoated conical metal wire.

the simulation results and experimental results demonstrate that the uncoated conical metal wire has strong field concentration. According to the experimental results, the field distributions around the conical tip were much stronger than those around the cylindrical tip. So from Fig. 3(b), we can find that the coated conical metal wire also has strong field concentration at the end tip, compared the uncoated conical metal wire. Due to its low loss and strong energy concentration, the coated conical metal wire has great promise for guiding terahertz wave to subwavelength volumes for near-field imaging, spectroscopy, and sensing application.

The electric field simulation results are shown in Fig. 4. Figs. 4(a), (b) and (c) show the magnitude of the electric field distribution (xy plane) of the coated conical metal wire, uncoated conical metal wire and coated cylindrical metal wire at 0.5 THz. It is very interesting that the terahertz energy is sharply concentrated around the coated conical metal wire and uncoated conical metal wire. The 2D images (xy plane) of the simulation spatial electric field distribution have symmetrical patterns. Red indicates high intensity and blue indicates low intensity. The figure shows that the electric field intensity around

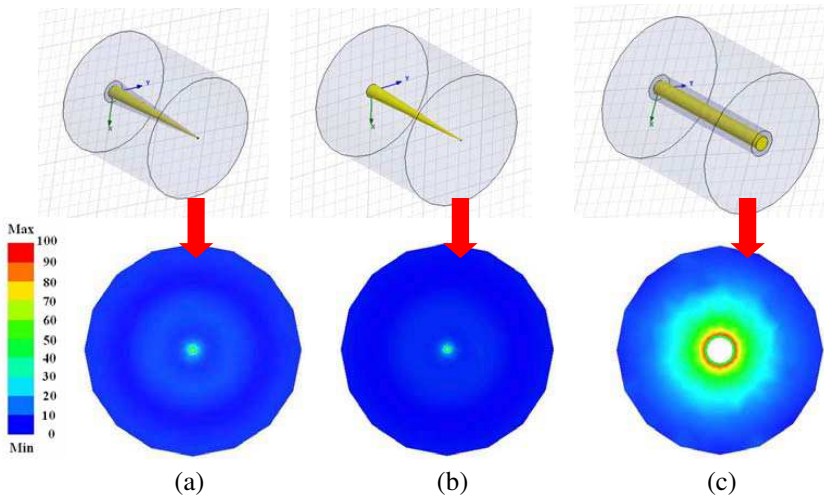


Figure 4. Simulation results of the electric field distribution on the xy plane. The white circle at the center of the field distribution indicates the surface of the metal wire. (a) The electric field distribution of the coated conical metal wire. (b) The electric field distribution of the uncoated conical metal wire. (c) The electric field distribution of the coated cylindrical metal wire.

the coated conical metal wire and uncoated conical metal wire were much larger than those around the coated cylindrical metal wire. Through the simulation results, it is clearly that both the coated conical metal wire and uncoated conical metal wire can realize stronger energy concentration. And from the results, we can find that around the coated conical metal wire, more energy concentrate around the dielectric layer. But around the uncoated conical metal wire, more energy concentrates around the surface of metal wire. Then it results in the increase of propagation attenuation. The simulation results are in agreement with the analysis results above. The energy concentration of the coated conical metal wire is very helpful for terahertz circuits.

4. COAXIAL PROBE TO CONICAL WIRE

Tapered transitions from a coaxial line to the coated conical metal wire and to the uncoated conical metal wire are simulated by using HFSS. Simulations are performed for transitions from a coaxial line with inner conductor radius $a = 250 \mu\text{m}$, radius of a dielectric coating $b = 300 \mu\text{m}$, and inner radius of outer conductor $c = 500 \mu\text{m}$ to a coated conical metal wire of dimensions of $a = 250 \mu\text{m}$ and $b = 500 \mu\text{m}$, $a_z = 25 \mu\text{m}$ and $b_z = 50 \mu\text{m}$, the total length is 15 mm. The dielectric material is Teflon: $\varepsilon_r = 2.05\varepsilon_0$, $\tan \delta = 0.001$ and metal is Copper: $5.8 \times 10^7 \text{S/M}$. Between the coaxial line and the conical wire, a taper is adopted. The simulation model is shown in Fig. 5. The radius of radiation boundary of the line is 4.5 mm and the length of radiation boundary is 10 mm. For reducing the simulation time, only a quarter of the transition is used. The simulation results are shown in Fig. 6. It is observed that the reflection coefficient is larger than 20 dB and the insertion loss is smaller than 5 dB from 0.1 THz to 0.5 THz. And from Fig. 6, we can find that the taper transition from the coaxial line to the coated conical metal wire has smaller insertion loss and larger reflection coefficient than the taper transition from the coaxial line to the uncoated conical metal wire at 0.1 THz–0.5 THz. In Ref. [44], a THz broadband transitions structure that coaxial probe to parallel-plate dielectric waveguide is proposed. By using HFSS, the coaxial-PPDW transitions (total length is 1 mm) insertion loss is less than 0.7 dB, and reflection coefficient is greater than 20 dB at 0.45–0.75 THz. Compared with the transition structure of [44], coaxial probe-to-conical wire demonstrates good propagation performance and wide bandwidth at lower THz frequency range.

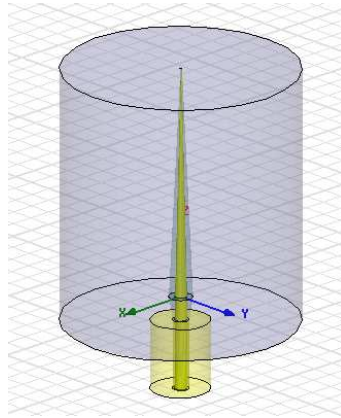


Figure 5. Simulation model of tapered transition from coaxial probe to coated conical metal wire.

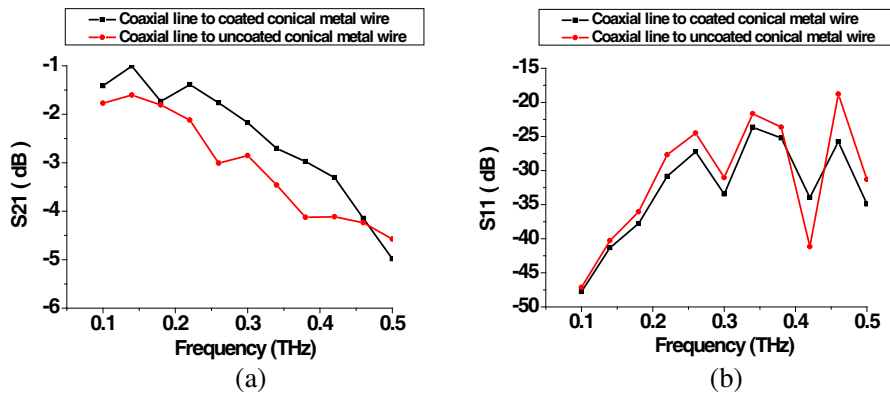


Figure 6. Simulation results of transitions from a coaxial probe to the coated conical metal wire and to the uncoated conical metal wire. (a) Reflection coefficient. (b) Insertion loss.

5. CONCLUSIONS

This paper present the results of a study on the characteristics of a conical metal wire with dielectric coating at 0.1–1 THz. The analysis results show that the theoretical calculation results agrees with the simulation ones. The conical metal wire with dielectric coating shows better energy concentration and superfocusing than the coated cylindrical metal wire due to the decrease of the end tip radius.

Because of the attracting of dielectric layer, energy concentrates on the surface of dielectric coating, and the proposed waveguide has lower propagation attenuation, compared with the uncoated conical metal wire. In this paper, a novel broadband transition from a coaxial probe to conical metal wire is designed at 0.1–0.5 THz. The results show that reflection coefficient is larger than 20 dB and that insertion loss is smaller than 5 dB from 0.1 THz to 0.5 THz. We believe that it is a very promising THz transition structure and very useful for the application of metal wire waveguide in the fields of imaging, sensing, and spectroscopy.

ACKNOWLEDGMENT

The work is supported by a key lab fund from National Key Laboratory of Monolithic Integrated Circuits and Modules (9140C1401010901).

REFERENCES

1. Siegel, P. H., "Terahertz technology in biology and medicine," *IEEE Trans. Microwave Theory Tech.*, Vol. 52, 2438–2447, 2004.
2. Nagel, M., P. Haring Bolivar, M. Brucherseifer, and H. Kurz, "Integrated THz technology for label-free genetic diagnostics," *Appl. Phys. Lett.*, Vol. 80, 154–156, 2002.
3. Schmuttenmaer, C. A., "Exploring dynamics in the far-Infrared with terahertz spectroscopy," *Chem. Rev.*, Vol. 104, 1759–1779, 2004.
4. Ogawa, Y., S. Hayashi, C. Otani, and K. Kawase, "Terahertz sensing for ensuring the safety and security," *PIERS Online*, Vol. 4, No. 3, 396–400, 2008.
5. Zhang, X. C., "Terahertz wave imaging: Horizons and hurdles," *Phys. Med. Biol.*, Vol. 47, 3667–3677, 2002.
6. Awad, M. M. and R. A. Cheville, "Transmission terahertz waveguide-based imaging below the diffraction limit," *Appl. Phys. Lett.*, Vol. 86, 1–3, 2005.
7. McGowan, R. W., G. Gallot, and D. Grischkowsky, "Propagation of ultrawideband short pulses of terahertz radiation through submillimeter-diameter circular waveguides," *Opt. Lett.* Vol. 24, No. 20, 1431–1433, 1999.
8. Gallot, G., S. P. Jamison, R. W. McGowan, and D. Grischkowsky, "Terahertz waveguides," *J. Opt. Soc. Am. B*, Vol. 17, No. 5, 851–863, 2000.

9. Zhou, Y. and S. Lucyszyn, "HFSSTM modeling anomalies with THz metal-pipe rectangular waveguide structures at room temperature," *PIERS Online*, Vol. 5, No. 3, 201–211, 2009.
10. Lucyszyn, S. and Y. Zhou, "Engineering approach to modeling frequency dispersion within normal metals at room temperature for THz applications," *Progress In Electromagnetics Research*, Vol. 101, 257–275, 2010.
11. Mendis, R. and D. Grischkowsky, "Plastic ribbon THz waveguides," *J. Appl. Phys.*, Vol. 88, 4449–4451, 2000.
12. Jamison, S. P., R. W. McGown, and D. Grischkowsky, "Single-mode waveguide propagation and reshaping of sub-ps terahertz pulses in sapphire fiber," *Appl. Phys. Lett.*, Vol. 76, 1987–1989, 2000.
13. Ponceca, Jr., C. S., R. Pobre, E. Estacio, N. Sarukura, et al., "Transmission of terahertz radiation using a microstructured polymer optical fiber," *Opt. Lett.*, Vol. 33, 902–904, 2008.
14. Han, H., H. Park, M. Cho, and J. Kim, "Terahertz pulse propagation in a plastic photonic crystal fiber," *Appl. Phys. Lett.*, Vol. 80, 2634–2636, 2002.
15. Chen, D. and H. Chen, "Highly birefringent low-Loss terahertz waveguide: Elliptical polymer tube," *Journal of Electromagnetic Waves and Applications*, Vol. 24, No. 11–12, 1553–1562, 2010.
16. Harrington, J. A., R. George, P. Pedersen, and E. Mueller, "Hollow polycarbonate waveguides with inner Cu coatings for delivery of terahertz radiation," *Opt. Express*, Vol. 12, 5263–5268, 2004.
17. He, X. Y. and H. X. Lu, "Investigation on propagation properties of terahertz waveguide hollow plastic fiber," *Opt. Fiber Technol.*, Vol. 12, 145–148, 2009.
18. Matsuura, Y. and E. Takeda, "Hollow optical fibers loaded with an inner dielectric film for terahertz broadband spectroscopy," *J. Opt. Soc. Am. B*, Vol. 25, 1949–1954, 2008.
19. Mendis, R. and D. Grischkowsky, "Undistorted guided-wave propagation of subpicosecond terahertz pulses," *Opt. Lett.*, Vol. 26, 846–848, 2001.
20. Coleman, S. and D. Grischkowsky, "A THz transverse electromagnetic mode two-dimensional interconnect layer incorporating quasi-optics," *Appl. Phys. Lett.*, Vol. 83, 3656–3658, 2003.
21. Zhang, H., S. Y. Tan, and H. S. Tan, "Experimental investigation on flanged parallel-plate dielectric waveguide probe for detection of conductive inclusions in lossy dielectric medium," *Journal of*

- Electromagnetic Waves and Applications*, Vol. 24, No. 5–6, 681–693, 2010.
22. Cheng, Q. and T. J. Cui, “Guided modes and continuous modes in parallel-plate waveguides excited by a line source,” *Journal of Electromagnetic Waves and Applications*, Vol. 21, No. 12, 1577–1587, 2007.
 23. Wang, K. and M. Mittleman, “Metal wires for terahertz wave guiding,” *Nature*, Vol. 432, 376–379, 2004.
 24. McGowan, R. W., G. Gallot, and D. Grischkowsky, “Propagation of ultra wideband short pulses of THz radiation through submillimeterdiameter circular waveguides,” *Opt. Lett.*, Vol. 24, 1431–1433, 1999.
 25. Wang, K. L. and D. M. Mittleman, “Dispersion of surface plasmon polaritons on metal wires in the terahertz frequency range,” *Phys. Rev. Lett.*, Vol. 96, 157401, 2006.
 26. Van der Valk, N. C. J. and P. C. M. Planken, “Effect of a dielectric coating on terahertz surface plasmon polaritons on metal wires,” *Appl. Phys. Lett.*, Vol. 87, 071106, 2005.
 27. Walther, M., M. R. Freeman, and F. A. Hegmann, “Metal-wire terahertz time-domain spectroscopy,” *Appl. Phys. Lett.*, Vol. 87, 261107, 2005.
 28. Haggmann, M. J., “Isolated carbon nanotubes as high-impedance transmission lines for microwave through terahertz frequencies,” *IEEE Trans. Nanotech.*, Vol. 4, 289–296, 2005.
 29. Jeon, T.-I., J. Zhang, and D. Grischkowsky, “THz Sommerfeld wave propagation on a single metal wire,” *Appl. Phys. Lett.*, Vol. 86, 161904, 2005.
 30. Ji, Y. B., E. S. Lee, J. S. Seok, T.-I. Jeon, M. H. Kwak, and K.-Y. Kwang, “Guidance properties of metal wire waveguide by terahertz pulse propagation,” *J. Korean Phys. Soc.*, Vol. 50, 1238–1242, 2007.
 31. Yang, F., J. R. Sambles, and G. W. Bradberry, “Long-range surface modes supported by thin films,” *Phys. Rev. B*, Vol. 44, 5855–5872, 1991.
 32. Goubau, G., “Surface waves and their application to transmission lines,” *J. Appl. Phys.*, Vol. 21, 1119–1128, 1950.
 33. Deibel, J. A., N. Berndsen, K. Wang, D. M. Mittleman, N. C. J. van der Valk, and P. C. M. Planken, “Frequency-dependent radiation patterns emitted by THz plasmons on finite length cylindrical metal wires,” *Opt. Express*, Vol. 14, 8772–8778, 2006.

34. Smorenburg, P. W., W. P. E. M. O. Root, and O. J. Luiten, "Direct generation of terahertz surface plasmon polaritons on a wire using electron bunches," *Phys. Rev. B*, Vol. 78, 115415, 2008.
35. Stockman, M. I., "Nanofocusing of optical energy in tapered plasmonic waveguides," *Phys. Rev. Lett.*, Vol. 93, 137404, 2004.
36. Liang, H., S. Ruan, and M. Zhang, "Terahertz surface wave propagation and focusing on conical metal wires," *Opt. Express*, Vol. 16, 18241–18248, 2008.
37. García-Vidal, "Terahertz surface plasmon-polariton propagation and focusing on periodically corrugated metal wires," *Phys. Rev. Lett.*, Vol. 97, 176805, 2006.
38. Vernon, K. C., D. K. Gramotnev, and D. F. P. Pile, "Adiabatic nanofocusing of plasmons by a sharp metal wedge on a dielectric substrate," *J. Appl. Phys.*, Vol. 101, 104312, 2007.
39. Awad, M., M. Nagel, and H. Kurz, "Tapered Sommerfeld wire terahertz near-field imaging," *Appl. Phys. Lett.*, Vol. 94, 051107, 2009.
40. Issa, N. A. and R. Guckenberger, "Fluorescence near metal tips: The roles of energy transfer and surface plasmon polaritons," *Opt. Express*, Vol. 15, 12131–12144, 2007.
41. King, M. J. and J. C. Wiltse, "Surface-wave propagation on coated and uncoated metal wires at millimeter wavelengths," *IRE Trans. Antennas Propag.*, Vol. 10, 246–254, 1962.
42. Pozar, D. M., *Microwave Engineering*, Wiley, New York, 2004.
43. Ji, Y. B., E. S. Lee, J. S. Jang, and T.-I. Jeon, "Enhancement of the detection of THz Sommerfeld wave using a conical wire waveguide," *Opt. Express*, Vol. 16, 271–278, 2008.
44. Ye, L. F., R. M. Xu, Z. H. Wang, and W. G. Lin, "A novel broadband coaxial probe to parallel plate dielectric waveguide transition at THz frequency," *Opt. Express*, Vol. 18, 21725–21731, 2010.